

**Classical excluded volumes of loosely bound light (anti)nuclei and their
chemical freeze-out in heavy ion collisions**

Boris E. Grinyuk

Bogolyubov Institute for Theoretical Physics, Metrologichna str. 14B, Kyiv 03680, Ukraine

Kyrill A. Bugaev

*Bogolyubov Institute for Theoretical Physics, Metrologichna str. 14B, Kyiv 03680, Ukraine
Department of Physics, Taras Shevchenko National University of Kyiv, 03022 Kiev, Ukraine
bugaev@th.physik.uni-frankfurt.de*

Violetta V. Sagun

*CFisUC, Department of Physics, University of Coimbra, Coimbra, 3004-516 Portugal
Bogolyubov Institute for Theoretical Physics, Metrologichna str. 14B, Kyiv 03680, Ukraine*

Oleksii I. Ivanytskyi

*CFisUC, Department of Physics, University of Coimbra, Coimbra, 3004-516 Portugal
Bogolyubov Institute for Theoretical Physics, Metrologichna str. 14B, Kyiv 03680, Ukraine*

Dmitry L. Borisjuk

Bogolyubov Institute for Theoretical Physics, Metrologichna str. 14B, Kyiv 03680, Ukraine

Anatoly S. Zhokhin

Bogolyubov Institute for Theoretical Physics, Metrologichna str. 14B, Kyiv 03680, Ukraine

Gennady M. Zinovjev

Bogolyubov Institute for Theoretical Physics, Metrologichna str. 14B, Kyiv 03680, Ukraine

David B. Blaschke

*Institute of Theoretical Physics, University of Wroclaw, Max Born Pl. 1. 50-204 Wroclaw,
Poland
Bogoliubov Laboratory of Theoretical Physics, JINR Dubna, Joliot-Curie Str. 6, 141980 Dubna,
Russia
National Research Nuclear University (MEPhI), Kashirskoe Shosse 31, 115409 Moscow, Russia*

Larissa V. Bravina

University of Oslo, POB 1048 Blindern, N-0316 Oslo, Norway

Evgeny E. Zabrodin

University of Oslo, POB 1048 Blindern, N-0316 Oslo, Norway

Skobeltsyn Institute of Nuclear Physics, Moscow State University, 119899 Moscow, Russia

Edward G. Nikonov

Laboratory for Information Technologies, JINR Dubna, Joliot-Curie str. 6, 141980 Dubna, Russia

Glennys Farrar

New York University, 726 Broadway, New York, New York, USA

Sonia Kabana

Instituto de Alta Investigación, Universidad de Tarapacá, Casilla 7D, Arica, Chile

Sergey V. Kuleshov

Departamento de Ciencias Físicas, Universidad Andres Bello, Sazié 2212, Piso 7, Santiago, Chile

Arkadiy V. Taranenko

National Research Nuclear University (MEPhI), Kashirskoe Shosse 31, 115409 Moscow, Russia

Received Day Month Year

Revised Day Month Year

From the analysis of light (anti)nuclei multiplicities that were measured recently by the ALICE collaboration in Pb+Pb collisions at the center-of-mass collision energy $\sqrt{s_{NN}} = 2.76$ TeV there arose a highly non-trivial question about the excluded volume of composite particles. Surprisingly, the hadron resonance gas model (HRGM) is able to perfectly describe the light (anti)nuclei multiplicities under various assumptions. Thus, one can consider the (anti)nuclei with a vanishing hard-core radius (as the point-like particles) or with the hard-core radius of proton, but the fit quality is the same for these assumptions. It is clear, however, that such assumptions are unphysical. Hence we obtain a formula for the classical excluded volume of loosely bound light nuclei consisting of A baryons. To implement a new formula into the HRGM we have to modify the induced surface tension concept to treat the hadrons and (anti)nuclei on the same footing. We perform a simultaneous analysis of hadronic and (anti)nuclei multiplicities measured by the ALICE collaboration. The HRGM with the induced surface tension allows us to verify different assumptions on the values of hard-core radii and different scenarios of chemical freeze-out of light (anti)nuclei. It is shown that the unprecedentedly high quality of fit $\chi^2_{tot}/dof \simeq 0.769$ is achieved, if the chemical freeze-out temperature of hadrons is about $T_h = 150$ MeV, while the one for all (anti)nuclei is $T_A = 174 - 175.2$ MeV.

Keywords: Hadron resonance gas; classical excluded volumes; composite clusters; induced surface tension.

PACS numbers: 25.75.Ag, 24.10.Pa

1. Introduction

After almost four decades of experiments on heavy ion collisions (HIC) which are aimed at the investigation of the phase diagram of quantum chromodynamics (QCD) it seems that only the low density phase of QCD known as the hadron

matter is well understood. However, a few puzzles emerged recently from the measurements of light (anti)nuclei yields made by the ALICE collaboration in Pb+Pb collisions at the center-of-mass collision energy $\sqrt{s_{NN}} = 2.76$ TeV.¹⁻³ The very fact that the light (anti)nuclei with binding energies of an order of a few MeV are produced at all in such violent collisions is very surprising. These data and their analysis performed within the simplest versions of the hadron resonance gas model (HRGM)^{4,5} faced HIC community with the following principal questions:⁴⁻⁶

- (i) What is the mechanism of production of deuterons (d), helium-3 (${}^3\text{He}$), helium-4 (${}^4\text{He}$) and hyper-triton (${}^3_{\Lambda}\text{H}$) and their antiparticles in relativistic HIC?
- (ii) What is the thermalization mechanism of such nuclear clusters?
- (iii) At what temperature does their chemical freeze-out (CFO) occurs?

Apparently these questions are closely related to each other, but to answer them one has to correctly answer the third of them first. The problem, however, appears due to the fact that the excluded volumes of light nuclei are not known. Therefore, the naive assumption of Ref. 5 that the hard-core radius of nuclei coincides with the proton one is absolutely unphysical. A more elaborate version of the HRGM⁷ based on the concept of induced surface tension^{8,9} demonstrated that the description of light (anti)nuclei can be achieved, if their CFO temperature is about 170 MeV, i.e. it is about 10% higher than the CFO temperature of hadrons.^{8,9}

However, the results of Ref. 7 were obtained using an approximate expression for the hard-core radius of light (anti)nuclei. Therefore, here we derive the correct expression for the classical excluded volumes of light (anti)nuclei and hyper-nuclei, modify the HRGM with induced surface tension and apply it to an analysis of the CFO temperature of such nuclei measured by the ALICE Collaboration.¹⁻³

The work is organized as follows. In Sect. 2 we remind the main ingredients of the HRGM based on the induced surface tension concept and briefly discuss the recent results obtained with HRGM with multicomponent hard-core repulsion among hadrons. Sect. 3 is devoted to a heuristic derivation of the new EoS which treats the hadrons and nuclear clusters on the same footing. In Sect. 4. we present our analysis of the ALICE data¹⁻³ on yields of nuclear clusters. Our conclusions are summarized in Sect. 5.

2. Hadron Resonance Gas Model with Induced Surface Tension

The most advanced and successful version of the HRGM with induced surface tension^{8,9} employs the Boltzmann statistics for all hadrons and (anti)nuclei. Note, that such an approximation is well justified at the CFO temperatures above 50-60 MeV and it essentially accelerates the fitting process. In the standard variables of grand canonical ensemble the HRGM with induced surface tension is a system of two coupled equations for the pressure p and for the induced surface tension coefficient

4

 Σ :

$$p = \sum_{k=1}^N p_k = T \sum_{k=1}^N \phi_k \exp \left[\frac{\mu_k - V_k p - S_k \Sigma}{T} \right], \quad (1)$$

$$\Sigma = \sum_{k=1}^N \Sigma_k = T \sum_{k=1}^N R_k \phi_k \exp \left[\frac{\mu_k - V_k p - S_k \alpha \Sigma}{T} \right]. \quad (2)$$

Here p_k and Σ_k are, respectively, the partial pressure and partial induced surface tension coefficient of the k -th sort of particle, while $V_k = \frac{4}{3}\pi R_k^3$ denotes its proper volume, $S_k = 4\pi R_k^2$ is its proper surface and R_k is its hard-core radius. The thermal density of particle of mass m_k , degeneracy g_k and chemical potential μ_k is $\phi_k(T) = g_k \int \frac{d^3p}{(2\pi\hbar)^3} \exp \left[-\frac{\sqrt{p^2 + m_k^2}}{T} \right]$.

The coefficient $\alpha = 1.25^{8,9}$ allows one to go beyond the second virial coefficient approximation and to correctly consider the high values of packing fractions up to $\eta \equiv \sum_k \frac{4}{3}\pi R_k^3 \rho_k \simeq 0.2 - 0.22$. It is highly nontrivial, that a single parameter α allows one to correctly reproduce the third and the fourth virial coefficient of the classical hard spheres.⁸⁻¹² Therefore, such a version of HRGM allows one to access the high values of particle number densities for which the HRGM based on the usual Van der Waals approximation¹³ is entirely wrong.

Using the partial values p_k and Σ_k one can write the particle number density of k -th sort of particle as

$$\rho_k \equiv \frac{\partial p}{\partial \mu_k} = \frac{1}{T} \cdot \frac{p_k a_{22} - \Sigma_k a_{12}}{a_{11} a_{22} - a_{12} a_{21}}, \quad (3)$$

where the coefficients a_{kl} are defined as

$$a_{11} = 1 + \frac{4}{3}\pi \sum_k R_k^3 \frac{p_k}{T}, \quad a_{12} = 4\pi \sum_k R_k^2 \frac{p_k}{T}, \quad (4)$$

$$a_{21} = \frac{4}{3}\pi \sum_k R_k^3 \frac{\Sigma_k}{T}, \quad a_{22} = 1 + 4\pi \sum_k R_k^2 \alpha \frac{\Sigma_k}{T}. \quad (5)$$

Then using Eqs. (3)-(5) one can find the absolute thermal yield $N_k^{th} = V \rho_k$ of particles and their thermal ratios $\mathcal{R}_{kl}^{th} = \frac{N_k^{th}}{N_l^{th}}$. For the known branchings $Br_{l \rightarrow k}$ of hadronic decays $l \rightarrow k$ one can determine the total yield of k -th sort of hadrons as

$$N_k^{tot} = V \left[\rho_k + \sum_{l \neq k} \rho_l Br_{l \rightarrow k} \right], \quad (6)$$

where V is the CFO volume. Since all details of the fitting process are well documented, we refer to the original works.^{8,9}

Another great advantage of the induced surface tension approach is that the number of equations for pressure p and induced surface tension coefficient Σ is always two and it does not depend on the number of different hard-core radii. This

advantage essentially reduces the CPU time of the fitting process, in the number of different hard-core radii is larger than 3.

It is necessary to stress that the high quality of description of the experimental multiplicities measured at AGS BNL, SPS CERN, RHIC BNL and LHC CERN accelerators was mainly achieved by the HRGM with the multicomponent hard-core repulsion,^{8,9,14–16} i.e. with several hard-core particles of hadrons. After the different hard-core radii of pions R_π , kaons R_K , of other mesons R_m and baryons R_b were implemented into the HRGM and used to describe the experimental hadronic multiplicities in Ref. 15, the HRGM became a reliable and extremely successful tool of HIC phenomenology to extract the parameters of chemical freeze-out of high energy nuclear collisions, i.e. the moment after which the inelastic reactions stop to exist, while the hadronic matter evolution is governed by the elastic reactions and the decays of resonances.¹³ The HRGM with multicomponent repulsion not only allowed us to achieve the highest quality of the hadronic multiplicity description with the smallest values of χ^2/dof being in the range between 0.96¹⁶ and 1.1,⁹ but it also allowed us for the first time to simultaneously describe the peaks in the collision energy dependence of K^+/π^+ and Λ/π^- ratios without spoiling the other hadronic ratios.¹⁵ Moreover, the HRGM with multicomponent repulsion allowed us to demonstrate that the γ_s -factor introduced in Ref. 17 to quantify the deviation of strange charge from chemical equilibrium is not necessary to describe the hadronic multiplicities, since they can be perfectly explained by the fact that the CFO of strange hadrons occurs on a separate hyper-surface compared to the hadrons consisting of u and d (anti)quarks.¹⁸ Note that the hypothesis of separate CFO of strange hadrons can be justified even, if the hadrons are treated as an ideal gas.¹⁹ More sophisticated scenarios of the CFO of strange particles can be found in Refs. 20, 21.

Furthermore, the successful description of the experimental hadronic multiplicities allowed us to uncover several irregularities in the energy dependencies of various thermodynamic and hydrodynamic quantities at CFO which were explained as possible experimental signals of two QCD phase transitions.^{22–26} The most remarkable irregularities include two sets of highly correlated quasi-plateaus found in^{22,23} which are located at the collision energy ranges $\sqrt{s_{NN}} = 3.8 - 4.9$ GeV and $\sqrt{s_{NN}} = 7.6 - 9.2$ GeV, and two peaks of trace anomaly $\delta = (\epsilon - 3p)/T^4$ observed at the maximal energy of each set of highly quasi-plateaus (here ϵ , p and T denote, respectively, the energy density of the system, its pressure and temperature). Using the HRGM with multicomponent repulsion it was possible to find out two strong peaks of the baryonic charge density located at $\sqrt{s_{NN}} = 4.9$ GeV and $\sqrt{s_{NN}} = 9.2$ GeV, i.e. exactly at the collision energies of the trace anomaly peaks.

The hydrodynamical signals, i.e. the highly correlated quasi-plateaus, in the low collision energy region were predicted a long time ago in Refs. 27, 28 as a manifestation of the mixed phase with the anomalous thermodynamic properties. Moreover, the generalized shock adiabat model^{27,28} allowed us to establish the one-to-one correspondence between the peak of trace anomaly δ at CFO and a

similar peak of δ at the generalized shock adiabat^{22,23} located at the boundary of the mixed and high density phases. Besides, at CFO the low energy signals are accompanied by the strong jumps of the pressure p and the effective number of degrees of freedom p/T^4 .²²⁻²⁴ The high energy irregularities are less pronounced and, hence, their interpretation was given later.^{25,26}

Very recently the advanced versions of HRGM helped us to estimate the number of the bosonic and fermionic degrees of freedom of the nearly massless matter that is created in HIC at the collision energies $\sqrt{s_{NN}} = 6.3 - 9.2$ GeV which, respectively, are $N_B \simeq 1520$ and $N_F \simeq 140$.²⁵ This finding allowed us to interpret the two sets of irregularities^{25,26} as the 1-st order phase transition from normal hadronic matter to the hadronic matter with partially restored chiral symmetry in the non-strange sector at $\sqrt{s_{NN}} = 3.8 - 4.9$ GeV and the 2-nd order phase transition (or a very weak one of the 1-st order) from nearly massless non-strange hadronic matter to quark gluon plasma (deconfinement) at $\sqrt{s_{NN}} = 9 - 10$ GeV. Remarkably, but a similar conclusion with very similar threshold collision energies of two QCD phase transitions was made in Refs. 29, 30 using the most advanced transport approach known as the Parton-Hadron-String-Dynamic-Model. Moreover, it is necessary to stress the idea that deconfinement phase transition is of 2-nd order was first suggested not by the lattice formulation of QCD, but by the QCD phenomenology in Refs. 31, 32.

From this extended reminder on the recent findings based on the HRGM with realistic hard-core repulsion one can see that essential improvement of the data description always led to a deep insight in the understanding of the QCD matter properties. Therefore, one can expect that the correct theoretical approach to the CFO of nuclear clusters in high energy HIC will provide us with extremely valuable information about the properties of matter from which such clusters are produced.

3. Excluded volumes of light nuclear clusters

The main problem with the excluded volumes of light (anti)nuclei consisting of A number of baryons ($2 \leq A \leq 4$) is not that they are loosely bound compared to the typical temperature $T \simeq 150 - 160$ MeV, but that they are the clusters themselves. Therefore, the usual Mayer procedure to calculate their cluster integrals and the excluded volumes cannot be used. However, the fact that the small nuclei of A baryons are roomy clusters, i.e. their radius $\mathcal{R}_A \sim 1.1(A)^{\frac{1}{3}}$ fm³³ is much larger than the maximal double hard-core radius of hadrons $2R_m \simeq 0.84$ fm,^{8,9} allows one to easily find out the desired excluded volume. Indeed, using this fact one can freely translate the hadron of hard-core radius R_h around each of the constituent (baryon of hard-core radius R_b) of a considered nuclear cluster without touching any other constituents inside this nucleus. Therefore, the resulting excluded volume (per particle) of a hadron and the nucleus of A baryons can be written as

$$b_{Ah} = A \frac{2}{3} \pi (R_b + R_h)^3, \quad (7)$$

where R_b is the hard-core radius of baryons. Unfortunately, one cannot use such excluded volumes in the system (1)-(5) and, therefore, our first task is to simplify Eq. (7).

From Eq. (7) one can find the equivalent hard-core radius R_{Ah}^{eq} of a pair Ah by equating two excluded volumes $\frac{2}{3}\pi(R_{Ah}^{eq})^3 = b_{Ah}$. Then we get the equivalent hard-core radius as

$$R_{Ah}^{eq} = A^{\frac{1}{3}}(R_b + R_h), \quad (8)$$

which can be used to determine the effective hard-core radius of a nucleus in a medium completely dominated by pions

$$R_A \simeq R_{A\pi}^{eq} - R_\pi \simeq A^{\frac{1}{3}}R_b + (A^{\frac{1}{3}} - 1)R_\pi \simeq A^{\frac{1}{3}}R_b. \quad (9)$$

Such an approximation is well justified by the fact that pions are the most abundant particles at ALICE collision energy and their hard-core radius $R_\pi \simeq 0.15$ fm^{8,9} is substantially smaller than $R_b = 0.365$ fm. Even for $A = 4$ the correction $(A^{\frac{1}{3}} - 1)R_\pi \leq 0.088$ fm neglected in Eq. (9) is very small compared to the effective hard-core radius of nuclei $R_A \simeq A^{\frac{1}{3}}R_b$. Nevertheless, to verify the validity of the HRGM (1)-(5) with the approximate expression (9) below we derive an alternative EoS which employs the true excluded volumes (7).

Our derivation of the alternative EoS is based on the heuristic approach of Ref. 34. In the variables of the grand canonical ensemble the pressure of the mixture of gases of hadrons and nuclear clusters can be written as (cluster expansion)³⁴

$$p \simeq T \sum_h \tilde{\phi}_h + T \sum_A \tilde{\phi}_A - T \sum_h \sum_{h'} \tilde{\phi}_h b_{hh'} \tilde{\phi}_{h'} - 2T \sum_h \sum_A \tilde{\phi}_h b_{hA} \tilde{\phi}_A. \quad (10)$$

The first two terms on the right hand side of Eq. (10) represent the pressure of ideal gases of hadrons and nuclei, while the other terms describe the hard-core repulsion between all particles. The excluded volumes of hadrons are given by the expression $b_{hh'} = \frac{2}{3}\pi(R_h + R_{h'})^3$, while the excluded volumes b_{hA} are defined by Eq. (7). The last term in Eq. (10) accounts for the excluded volumes $b_{Ah} = b_{hA}$ as well, but it is doubled to shorten the notations. Evidently, the hard-core repulsion between two nuclear clusters can be neglected due to their low particle number density.

To simplify the evaluation in Eq. (10) we introduced the particle number density of the ideal Boltzmann gas of sort n as

$$\tilde{\phi}_n = g_n \int \frac{dk^3}{(2\pi\hbar)^3} \exp \left[\frac{\mu_n - \sqrt{p^2 + m_n^2}}{T} \right]. \quad (11)$$

Substituting into Eq. (10) the expressions for the excluded volumes, one finds

$$\begin{aligned}
p &\simeq T \sum_h \tilde{\phi}_h + T \sum_A \tilde{\phi}_A - T \sum_h \sum_{h'} \tilde{\phi}_h \frac{2}{3} \pi [R_h^3 + 3R_h^2 R_{h'} + 3R_h R_{h'}^2 + R_{h'}^3] \tilde{\phi}_{h'} - \\
&- T \sum_h \sum_A \tilde{\phi}_h \frac{4}{3} \pi [R_h^3 + 3R_h^2 R_b + 3R_h R_b^2 + R_b^3] A \tilde{\phi}_A \simeq \\
&\simeq T \sum_h \tilde{\phi}_h + T \sum_A \tilde{\phi}_A - T \sum_h \tilde{\phi}_h \frac{4}{3} \pi R_h^3 \left[\sum_{h'} \tilde{\phi}_{h'} \right] - T \sum_h \tilde{\phi}_h 4\pi R_h^2 \left[\sum_{h'} R_{h'} \tilde{\phi}_{h'} \right] - \\
&- T \sum_h \tilde{\phi}_h \frac{4}{3} \pi R_h^3 \left[\sum_A A \tilde{\phi}_A \right] - T \sum_h \tilde{\phi}_h 4\pi R_h^2 \left[\sum_A R_b A \tilde{\phi}_A \right] - \\
&- T \sum_A \tilde{\phi}_A \left[\frac{4}{3} \pi R_b^3 A \left[\sum_{h'} \tilde{\phi}_{h'} \right] + 4\pi R_b^2 A \left[\sum_{h'} R_{h'} \tilde{\phi}_{h'} \right] \right]. \tag{12}
\end{aligned}$$

Regrouping in Eq. (13) the terms with partial pressure of ideal gas $p_i \sim T\tilde{\phi}_i$ and the partial coefficient of induced surface tension of ideal gas $\Sigma_i \sim TR_i\tilde{\phi}_i$, where $R_i = \{R_h, AR_b\}$, one can write

$$\begin{aligned}
p &\simeq T \sum_h \tilde{\phi}_h \times \\
&\times \left[1 - \frac{4}{3} \pi R_h^3 \left(\sum_{h'} \tilde{\phi}_{h'} + \sum_A A \tilde{\phi}_A \right) - 4\pi R_h^2 \left(\sum_{h'} R_{h'} \tilde{\phi}_{h'} + \sum_A R_b A \tilde{\phi}_A \right) \right] + \\
&+ T \sum_A \tilde{\phi}_A \left[1 - \frac{4}{3} \pi R_b^3 A \left(\sum_{h'} \tilde{\phi}_{h'} \right) - 4\pi R_b^2 A \left(\sum_{h'} R_{h'} \tilde{\phi}_{h'} \right) \right]. \tag{14}
\end{aligned}$$

Recalling that at low particle number densities the pressure can be approximated by the ideal gas term, one can rewrite Eq. (14) as the following system

$$\begin{aligned}
p &\simeq T \sum_h \tilde{\phi}_h \left[1 - \frac{4}{3} \pi R_h^3 \left(\frac{p}{T} + \sum_A (A-1) \tilde{\phi}_A \right) - 4\pi R_h^2 \frac{\Sigma}{T} \right] \\
&+ T \sum_A \tilde{\phi}_A \left[1 - \frac{4}{3} \pi R_b^3 A \left(\frac{p}{T} + \sum_A (A-1) \tilde{\phi}_A \right) - 4\pi R_b^2 A \frac{\Sigma}{T} \right], \tag{15}
\end{aligned}$$

$$\Sigma \simeq T \left[\sum_{h'} R_{h'} \tilde{\phi}_{h'} + \sum_A R_b A \tilde{\phi}_A \right]. \tag{16}$$

Apparently we can safely neglect the small term $T \sum_A (A-1) \tilde{\phi}_A$ compared to the pressure p in Eq. (15). Furthermore, the following modification of the particle number densities $\tilde{\phi}_h$ and $\tilde{\phi}_A$

$$\tilde{\phi}_h \rightarrow \tilde{\phi}_h \exp \left[-\frac{4}{3} \pi R_h^3 \frac{p}{T} - \alpha 4\pi R_h^2 \frac{\Sigma}{T} \right], \tag{17}$$

$$\tilde{\phi}_A \rightarrow \tilde{\phi}_A \exp \left[-\frac{4}{3} \pi R_b^3 A \frac{p}{T} - \alpha 4\pi R_b^2 A \frac{\Sigma}{T} \right], \tag{18}$$

in Eq. (16) will change only the higher order terms of cluster expansion which can be corrected later on by proper choice of parameter α .¹² Taking this into account, now we can extrapolate the system (15), (16) to high densities as

$$p_v = T \sum_h \tilde{\phi}_h \exp \left[-\frac{4}{3} \pi R_h^3 \frac{p_v}{T} - 4\pi R_h^2 \frac{\Sigma_v}{T} \right] + T \sum_A \tilde{\phi}_A \exp \left[-\frac{4}{3} \pi R_b^3 A \frac{p_v}{T} - 4\pi R_b^2 A \frac{\Sigma_v}{T} \right], \quad (19)$$

$$\Sigma_v = T \sum_h R_h \tilde{\phi}_h \exp \left[-\frac{4}{3} \pi R_h^3 \frac{p_v}{T} - \alpha 4\pi R_h^2 \frac{\Sigma_v}{T} \right] + T \sum_A R_b A \tilde{\phi}_A \exp \left[-\frac{4}{3} \pi R_b^3 A \frac{p_v}{T} - \alpha 4\pi R_b^2 A \frac{\Sigma_v}{T} \right], \quad (20)$$

where the parameter $\alpha = 1.245$ is introduced to account for higher order classical virial coefficients as it is shown in Refs. 8,9,12. The subscript v in the quantities p_v and Σ_v of the system (19), (20) is introduced to indicate that it is obtained from the excluded volume expression (7) of nuclear cluster of A baryons and a hadron h . This system can be obtained more rigorously by the Laplace transform method in a spirit of Ref. 35, but such a derivation is even more complicated than the one presented above.

The expressions (3)-(5) can be used to calculate the particle number densities of nuclear clusters for the system (19), (20), if one makes the following replacements $R_A^2 \rightarrow AR_b^2$ and $R_A^3 \rightarrow AR_b^3$ in Eqs. (4)-(5).

Rewriting the systems (1), (2) in terms of the effective radius of the nuclear cluster (9), one obtains

$$p_r = T \sum_h \tilde{\phi}_h \exp \left[-\frac{4}{3} \pi R_h^3 \frac{p_r}{T} - 4\pi R_h^2 \frac{\Sigma_r}{T} \right] + T \sum_A \tilde{\phi}_A \exp \left[-\frac{4}{3} \pi R_b^3 A \frac{p_r}{T} - 4\pi R_b^2 A^{\frac{2}{3}} \frac{\Sigma_r}{T} \right], \quad (21)$$

$$\Sigma_r = T \sum_h R_h \tilde{\phi}_h \exp \left[-\frac{4}{3} \pi R_h^3 \frac{p_r}{T} - \alpha 4\pi R_h^2 \frac{\Sigma_r}{T} \right] + T \sum_A R_b A^{\frac{1}{3}} \tilde{\phi}_A \exp \left[-\frac{4}{3} \pi R_b^3 A \frac{p_r}{T} - \alpha 4\pi R_b^2 A^{\frac{2}{3}} \frac{\Sigma_r}{T} \right], \quad (22)$$

where we introduced the subscript r in the functions p_r and Σ_r to signify the fact that it is obtained using an effective hard-core radius of the nuclear cluster (9).

Comparing the systems (19), (20) and (21), (22), one can see that only the eigen volumes of nuclear clusters are the same, while the eigen surface $4\pi R_b^2 A$ and the eigen radius $R_b A$ of a nucleus of A baryons of the system (19), (20) are larger than the corresponding quantities of the system (21), (22). Therefore, for the same values of T and $\{\mu_k\}$ the partial pressure of such nuclear cluster and, consequently, its

particle number density, will be smaller for the system (19), (20). In other words, to obtain the same particle number density of nuclear clusters of A baryons the temperature or chemical potentials of the system (19), (20) should be larger than for the system (21), (22). Nevertheless, since the system (21), (22) was obtained under the reasonable approximation, then for the pion dominated hadronic matter the results obtained from the EoS (21), (22) should be very similar to the ones found from the EoS (19), (20). This will be our guideline for the analysis of ALICE data.¹⁻³

4. Details of fitting procedure

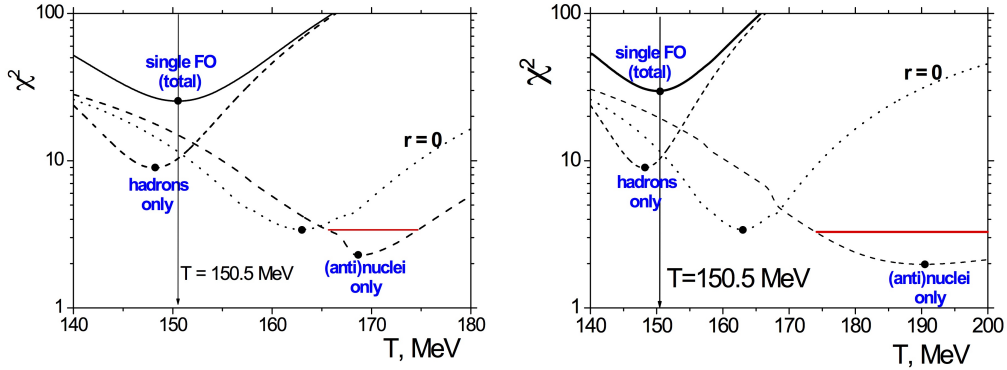


Fig. 1. **Left panel.** χ^2 as a function of the CFO temperature T for the ALICE data: hadrons only (short dash curve), nuclear clusters only for the EoS (21), (22) (short dashed curve) and their sum (solid curve). For a comparison the χ^2_A of nuclear clusters with the vanishing size is shown by the dotted curve. Horizontal bar on top of the χ^2 minimum of nuclear clusters shows the deviations that correspond to $\min(\chi^2) + 1$. **Right panel.** Same as in the left panel, but for the EoS (19), (20).

Two formulations of the HRGM with induced surface tension, i.e. R- and V-approaches, described in the preceding section are applied to describe the whole set of the ALICE data measured at $\sqrt{s_{NN}} = 2.76$ TeV. Since the hadronic multiplicities are very well described by the HRGM with the induced surface tension with $\chi_h^2/dof \simeq 10.7/(11 - 1) \simeq 1.07^9$ here we do not discuss the results of this analysis. The most important assumption used to analyze the ALICE data measured at $\sqrt{s_{NN}} = 2.76$ TeV is that all chemical potentials are set to zero.^{8,9} More details describing the HRGM, the analyzed data and the fitting process can be found in Refs. 8, 9. Hence, here our main attention is paid to the fitting of the nuclear clusters data¹⁻³ for the centrality 0 – 10%.

First we discuss the traditional approach in which it is assumed that the CFO occurs for all particles simultaneously, i.e. hadrons and (anti)nuclei, are freezing

out from a single hyper-surface of CFO. Then the total $\chi_{tot}^2(V)$ of such a model (M1 hereafter) is as follows

$$\chi_{tot}^2(V) = \chi_h^2 + \chi_A^2(V) = \sum_{\text{pairs } k,l} \left[\frac{\mathcal{R}_{kl}^{theo} - \mathcal{R}_{kl}^{exp}}{\delta \mathcal{R}_{kl}^{exp}} \right]^2 + \sum_A \left[\frac{\rho_A(T)V - N_A^{exp}}{\delta N_A^{exp}} \right]^2. \quad (23)$$

Here χ_h^2 and χ_A^2 denote, respectively, the properly normalized mean deviation squared for hadrons and (anti)nuclei. According to Refs. 8,9 the hadronic part of $\chi_{tot}^2(V)$ contains only the ratios of hadronic multiplicities \mathcal{R}_{kl} , since in this case one does not need the CFO volume for fitting. Such a fitting procedure has several advantages and was successfully used in our previous publications.^{8,9,15,16,18,21,25,26} It, however, is inconsistent with the (anti)nuclei part of $\chi_{tot}^2(V)$ which depends on the thermal densities of (anti)nuclei of A (anti)baryons and the CFO volume V . The simplest way to determine the CFO volume V is to use the maximum likelihood method, i.e. for each value of CFO temperature T to find the minimum of $\chi_{tot}^2(V)$ with respect to the CFO volume V and to determine the function $V(T)$ from the equation $\frac{\partial \chi_{tot}^2(V)}{\partial V} = 0$. Then the model has two fitting parameters, namely the CFO temperature and volume. We verified that another way of fitting by introducing the ratios of (anti)nuclei to the multiplicity of π^+ -mesons, like it is done for the hadronic ratios, provides practically the same result for the CFO temperature, but, unfortunately, the resulting error for the ratio of multiplicities is larger and, hence, the resulting χ_{tot}^2 is slightly smaller.

As one can see from Fig. 1 the minimum of χ_{tot}^2 for the M1 is achieved at the same CFO temperature $T_{M1} \simeq 150.5 \pm 6$ MeV for both EoS. This is a consequence of the fact that the main contribution to χ_{tot}^2 is defined by the hadrons, since it strongly increases with increasing T_{M1} . This can also be seen from the both panels of Fig. 1. However, the model M1R defined by the EoS (21), (22) provides slightly better value of $\chi_{tot}^2/dof|_{M1R} \simeq (10.1 + 15)/(11 + 8 - 2) = 25.1/17 \simeq 1.476$, where 11 is the number of fitted hadronic ratios, 8 is the number of analyzed data point for the nuclear clusters. For the model M1V defined by the EoS (19), (20) one finds that $\chi_{tot}^2/dof|_{M1V} \simeq (10.1 + 21)/(11 + 8 - 2) = 31.1/17 \simeq 1.83$. Thus, we got a very strange and surprising result that the more elaborate model describes the same set of data somewhat worse than the approximative one.

However, if one analyzes the contributions of χ_h^2 and $\chi_A^2(V)$ separately (see Fig. 1), then one finds that their local minima are located at rather different temperatures, but the sum of χ_h^2 and $\chi_A^2(V)$ has a minimum which is located more close to the minimum of χ_h^2 ! Moreover, from Fig. 1 one can see that $\chi_A^2(V)$ has a deep minimum even for the vanishing size of nuclear clusters, i.e. an existence of such a minimum is a generic feature of the advanced versions of HRGM. Hence, we concluded that it is worth to verify the hypothesis of separate CFO of hadrons and nuclear clusters.⁷ Hereafter such a model is called M2. In this case there are three fitting parameters, namely the CFO temperature of hadrons T_h , the one of nuclear clusters T_A and the CFO volume V of nuclei. For the EoS (21), (22) one finds that

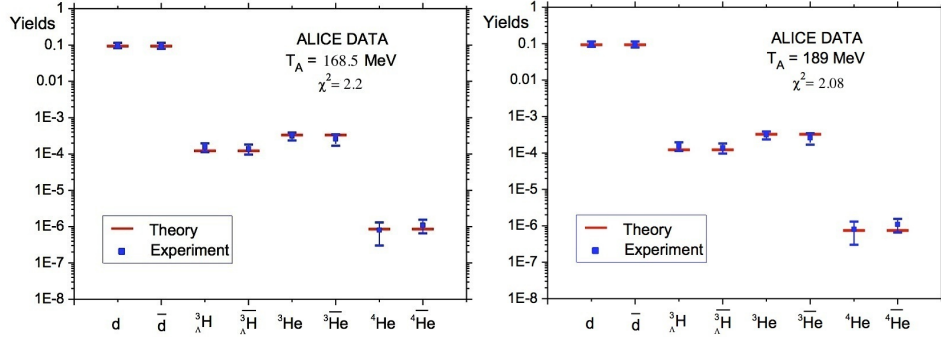


Fig. 2. **Left panel.** The yields of nuclear clusters at the CFO temperature $T = 168.5$ MeV which corresponds to $\min \chi_A^2(V)$ for the EoS (21), (22): the ALICE data (symbols) vs. theoretical description (bars). **Right panel.** Same as in the left panel, but for the EoS (19), (20). $\min \chi_A^2(V)$ corresponds to the CFO temperature $T = 189$ MeV.

$T_A^{M2R} \simeq 168.5 - 2.6 + 6.7$ MeV and $\chi_{tot}^2/dof|_{M2R} \simeq (9.1 + 2.2)/(11 + 8 - 3) = 11.3/16 \simeq 0.706$. In other words, compared to the M1R the mean deviation squared per number of degrees of freedom of M2R decreased on 50%!

A similar hypothesis verified with the EoS (19), (20) gives us $T_A^{M2V} \simeq 189 - 15 + 38$ MeV and $\chi_{tot}^2/dof|_{M2V} \simeq (9.1 + 2.08)/(11 + 8 - 3) = 11.18/16 \simeq 0.699$. The latter value is very close to the value $\chi_{tot}^2/dof|_{M2R}$ and, hence, we do not face the problem of M1. Moreover, as one can see from Fig. 2 an excellent fit quality provided by two different EoS is very similar. However, at first glance we face two new problems, namely that the CFO temperatures of nuclear clusters differ essentially from each other and that the CFO temperature T_A^{M2V} is somewhat larger than the cross-over temperature $T_{co} \simeq 147 - 170$ MeV predicted by the lattice formulation of QCD at vanishing value of the baryonic chemical potential.^{38,39}

Considering the cross-over temperature value one should remember that the lattice formulation of QCD predicts the temperature of an infinite system. In HIC, on contrary, the formed systems are small and they have boundary with the vacuum. Therefore, it is not surprising that the temperature of small systems created in HIC may be higher than the ones predicted by the lattice formulation of QCD. The validity of this statement can be seen from the values of CFO temperature found for the RHIC highest collision energies which are about 170-175 MeV.^{4,9,36,37}

The problem with different values of CFO temperatures found for M2R and M2V can also be resolved easily. Indeed, comparing the left and right panels of Fig. 1 one can see that there is a region of CFO temperatures at which the shallow minima of $\chi_A^2|_{M2R}$ and $\chi_A^2|_{M2V}$ obeying the following inequalities $\chi_A^2|_{M2R} \leq \min(\chi_A^2|_{M2R}) + 1$ and $\chi_A^2|_{M2V} \leq \min(\chi_A^2|_{M2V}) + 1$ do overlap. Note that exactly these inequalities are used to determine the most probable range of CFO temperature. Hence there is a narrow region of CFO temperatures $T_A^{M2} \in [174; 175.2]$ MeV where both EoS discussed above provide a fit of ALICE data of very similar quality. One can estimate

the total quality of the fit for $T_A^{M2} \in [174; 175.2]$ MeV and get $\chi_{tot}^2/dof|_{M2} \simeq (9.1 + 3.2)/(11 + 8 - 3) = 12.3/16 \simeq 0.769$ which is only about 10% larger than the best fit of the M2 found above. Thus, both EoS describing the mixture of hadrons and nuclear clusters agree well with each other for the CFO temperature of nuclear clusters $T_A^{M2} \simeq 174.6 \pm 0.6$ MeV. This CFO temperature is in remarkable agreement with the CFO temperature of hadrons found for the highest RHIC energies.^{4, 9, 36, 37}

5. Conclusions

In this work we found the classical excluded volumes of roomy clusters which can be used to describe the yields of such nuclear clusters as deuterons, helium-3, helium-4 and hyper-triton and their antiparticles. From the obtained expression (7) we deduced an approximate formula (9) for the effective hard-core radius of nuclear clusters for a pion dominated medium. The main advantages of the formula (9) are its simplicity and that it does not require an essential modification of the HRGM based on the induced surface tension concept (R-approach) developed in Refs. 8, 9. However, to verify the validity of such an approach we heuristically derived the novel HRGM with induced surface tension (V-approach) which employs the true classical excluded volumes of roomy clusters. By construction the both approaches should provide similar results for a pion dominated medium.

Using these two approaches we analyzed the ALICE data¹⁻³ on the yields of nuclear clusters. Our first analysis (the model M1) is based on the traditional assumption that the CFO of hadrons and nuclear clusters occurs at the same hyper-surface and, therefore, the CFO temperature and volume are the fitting parameters of such a model. Although the found CFO temperatures of R- and V-approaches, i.e. the models M1R and M1V, agree well with each other, we got a paradoxical result, namely that the quality of the description of approximate approach $\chi_{tot}^2/dof|_{M1R} \simeq 1.476$ is essentially higher than the one $\chi_{tot}^2/dof|_{M1V} \simeq 1.83$ obtained by a more elaborate V-approach. Thus, we faced an alternative: (1) either to claim that the nuclear clusters cannot be accurately described by the advanced V-approach and, hence, the description of the nuclear clusters obtained in the over-simplified versions of the HRGM⁴⁻⁶ is just a kind of illusion, or (2) to abandon the traditional assumption of a single CFO of hadrons and nuclear clusters.

A close inspection of the $\chi_A^2(V(T))$ as a function of CFO temperature T showed us that $\chi_A^2(V(T))$ of nuclear clusters has a deep minimum located at higher temperature than the CFO one of M1. Hence we verified the model M2 in which the CFO of nuclear clusters occurs separately from CFO of hadrons. As it was argued a long time ago,^{40, 41} at temperatures above the pion mass one can naturally expect an early and simultaneous chemical and kinetic freeze-out for heavy particles, which do not produce the resonances with pions. In Refs. 40, 41 the validity of such a hypothesis was demonstrated for Ω hyperons and J/ψ and ψ' mesons. Later on it was shown¹⁸⁻²¹ that at the collision energies above SPS ones the CFO of strange hadrons occurs separately at temperatures higher than for the non-strange ones.

Thus, our M2 is a natural extension of an early CFO hypothesis. Moreover, intuitively it is clear that the compact objects as hadrons and the extended ones as the nuclear clusters may require different conditions of formation and, hence, our M2 is in line with this expectation.

In the M2 there appears an additional fitting parameter compared to the M1, i.e. the CFO temperature of nuclear clusters T_A . Then we got an opposite situation than for the M1 that $\chi^2_{tot}/dof|_{M2R} \simeq 0.706$ and $\chi^2_{tot}/dof|_{M2V} \simeq 0.699$ of R- and V-approaches agree well with each other, but their CFO temperatures are rather different. As one can see from Fig. 2 both versions of the M2 provide an unprecedentedly accurate description of nuclear clusters' yields. This fact motivated us to resolve the problem with different values of CFO temperature of nuclear clusters. It turns out that within a narrow region of CFO temperatures $T_A^{M2} = 174 - 175.2$ MeV the both approaches agree very well with each other, as it was expected in the first place. Moreover, we found that in this narrow region of CFO temperatures the description of both approaches is still unprecedentedly accurate with $\chi^2_{tot}/dof|_{M2} \simeq 0.769$. These findings are of principal importance for the HIC phenomenology, since they may shed the light on the mechanism of early freeze-out, both the chemical and the kinetic one, of nuclear clusters and shake the validity of fits obtained with oversimplified versions of the HRGM.

Acknowledgements. The authors are thankful to O. V. Vitiuk and E. S. Zhrebtsova for fruitful discussions and helpful comments. K.A.B., B.E.G., V.V.S., O.I.I. and G.M.Z. acknowledge the partial support by the Program of Fundamental Research in High Energy and Nuclear Physics launched by the Section of Nuclear Physics of the NAS of Ukraine. V.V.S. and O.I.I. are thankful for the support by the Fundação para a Ciência e Tecnologia (FCT), Portugal, under the project UID/FIS/04564/2019. The work of O.I.I. was supported by the project CENTRO-01-0145-FEDER-000014 through CENTRO2020 program, and POCI-01-0145-FEDER-029912 with financial support from POCI, in its FEDER component, and by the FCT/MCTES budget through national funds (OE). The work of L.V.B. and E.E.Z. was supported by the Norwegian Research Council (NFR) under grant No. 255253/F50 - CERN Heavy Ion Theory. L.V.B. and K.A.B. thank the Norwegian Agency for International Cooperation and Quality Enhancement in Higher Education for financial support, grant 150400-212051-120000 "CPEA-LT-2016/10094. A.V.T. acknowledges partial support from RFBR under grant No. 18-02-40086 and from the Ministry of Science and Higher Education of the Russian Federation Project No 0723-2020-0041. D.B.B. received funding from the RFBR under grant No. 18-02-40137. The authors are thankful to the COST Action CA15213 for supporting their networking.

References

1. ALICE Collaboration (J. Adam *et al.*), *Phys. Rev. C* **93**, 024917 (2016).
2. ALICE Collaboration (L. Ramona *et al.*), *AIP Conf. Proc.* **1701**, (1) 080009 (2016).
3. ALICE Collaboration (J. Adam *et al.*), *Phys. Lett. B* **754**, 360 (2016).

4. J. Cleymans, S. Kabana, I. Kraus, H. Oeschler, K. Redlich and N. Sharma, *Phys. Rev. C* **84** 054916 (2011).
5. J. Stachel, A. Andronic, P. Braun-Munzinger and K. Redlich, *J. Phys. Conf. Ser.* **509**, 012019 (2014).
6. P. Braun-Munzinger and B. Dönigus, *Nucl. Phys. A* **987**, 144 (2019).
7. K. A. Bugaev *et al.*, *J. of Phys. Conf. Series* **1390**, 012038 (2019).
8. K. A. Bugaev *et al.*, *Nucl. Phys. A* **970**, 133 (2018).
9. V. V. Sagun *et al.*, *Eur. Phys. J. A* **54**, 100 (2018).
10. A. I. Ivanytskyi, K. A. Bugaev, V. V. Sagun, L. V. Bravina and E. E. Zabrodin, *Phys. Rev. C* **97**, 064905 (2018).
11. K. A. Bugaev, A. I. Ivanytskyi, V. V. Sagun, E. G. Nikonov and G. M. Zinovjev, *Ukr. J. Phys.* **63**, 863 (2018).
12. K. A. Bugaev, *Eur. Phys. J. A* **55**, 215 (2019);
13. A. Andronic, P. Braun-Munzinger and J. Stachel, *Nucl. Phys. A* **772**, 167 (2006) and references therein.
14. K. A. Bugaev *et al.*, *Universe* **5**, 00063 (2019).
15. K. A. Bugaev, D. R. Oliinychenko, A. S. Sorin and G. M. Zinovjev, *Eur. Phys. J. A* **49**, 30 (2013).
16. V. V. Sagun, *Ukr. J. Phys.* **59**, 755 (2014).
17. J. Rafelski, *Phys. Lett. B* **262**, 333 (1991).
18. K. A. Bugaev *et al.*, *Europhys. Lett.* **104**, 22002 (2013).
19. S. Chatterjee, R.M. Godbole and S. Gupta, *Phys. Lett. B* **727**, 554 (2013).
20. S. Chatterjee *et al.*, *Adv. High Energy Phys.* **2015**, 349013 (2015).
21. K. A. Bugaev *et al.*, *Ukr. J. Phys.* **61**, 659 (2016).
22. K. A. Bugaev *et al.*, *Phys. Part. Nucl. Lett.* **12**, 238 (2015).
23. K. A. Bugaev *et al.*, *Eur. Phys. J. A* **52**, 175 (2016).
24. K. A. Bugaev *et al.*, *Eur. Phys. J. A* **52**, 227 (2016).
25. K. A. Bugaev *et al.*, *Phys. Part. Nucl. Lett.* **15**, 210 (2018).
26. K. A. Bugaev *et al.*, *EPJ Web of Conferences* **204**, 03001 (2019).
27. K. A. Bugaev, M. I. Gorenstein, B. Kämpfer and V. I. Zhdanov, *Phys. Rev. D* **40**, 2903 (1989).
28. K. A. Bugaev, M. I. Gorenstein and D. H. Rischke, *JETP Lett.* **52**, 1121 (1990).
29. W. Cassing, A. Palmese, P. Moreau, and E. L. Bratkovskaya, *Phys. Rev. C* **93**, 014902 (2016).
30. A. Palmese *et al.*, *Phys. Rev. C* **94**, 044912 (2016).
31. S. Kabana and P. Minkowski, *New J. Phys.* **3**, 4 (2001).
32. S. Kabana and P. Minkowski, *Int. J. Mod. Phys. A* **26**, 3035 (2011).
33. A. Bohr and B. Mottelson, *Nuclear Structure*, vol. 1 (Benjamin, New York, 1969).
34. V. V. Sagun, A. I. Ivanytskyi, K. A. Bugaev and I. N. Mishustin, *Nucl. Phys. A* **924**, 24 (2014).
35. N. S. Yakovenko, K. A. Bugaev, L.V. Bravina and E. E. Zabrodin, arXiv:1910.04889 [nucl-th] p. 1-13.
36. S. Chatterjee *et al.*, *Adv. High Energy Phys.* 2015, 349013 (2015).
37. A. Andronic, P. Braun-Munzinger, K. Redlich and J. Stachel, *J. Phys. Conf. Ser.* **779**, 012012 (2017).
38. Wuppertal-Budapest Collaboration (S. Borsanyi *et al.*), *JHEP* **1009**, 073 (2010).
39. HotQCD Collaboration (A. Bazavov *et al.*), *Phys. Rev. D* **90**, 094503 (2014).
40. K. A. Bugaev, M. Gazdzicki and M. I. Gorenstein, *Phys. Lett. B* **523**, 255 (2001).
41. M. I. Gorenstein, K. A. Bugaev and M. Gazdzicki, *Phys. Rev. Lett.* **88**, 132301 (2002).